Model-based nonlinear dynamic optimisation for the optimal flow rate of vanadium redox flow batteries

Hao Wang*a, S. Ali Pourmousavia, Wen L. Soonga, Xinan Zhangb, Nesimi Ertugrula, Bingyu Xiongc

^aSchool of Electrical & Electronic Engineering, The University of Adelaide, Australia ^bSchool of Engineering, The University of Western Australia, Australia ^cSchool of Automation, Wuhan University of Technology, China

Abstract

The control of the electrolyte flow rate is crucial to ensure the efficient operation of a vanadium redox flow battery (VRFB) system. In this paper, a model-based nonlinear dynamic optimisation (MNDO) method is proposed and implemented in MATLAB/Simulink to study the optimal flow rate under constant current (CC) and constant current-constant voltage (CC-CV) charging methods for a VRFB. A 5kW/3kWh VRFB system is considered to investigate the feasibility and accuracy of the established model. System efficiency is the optimisation objective in this study, where all case studies are carried out within 15% to 85% state of charge (SOC). The simulation results show that the proposed method enhanced battery performance by improving the overall VRFB system efficiency under different charging methods. Furthermore, the simulation results show that the CC-CV method is more energy-efficient than the CC method but requires more charging time. An in-depth analysis is carried out to discuss the underlying merits of the proposed method in balancing the losses caused by the concentration overpotential and pump energy consumption in a varying power environment. Moreover, further analyses are carried out to highlight the merits of the CC-CV charging method in saving energy while charging and reducing system imbalance. Finally, a 2D lookup table is designed based on the results from the proposed MNDO method that offers a practical controller of the electrolyte flow rate without requiring excessive computational resources. The performance of the 2D lookup table has been evaluated within 100 charging/discharging cycles. It achieves a system efficiency gain of up to 1.48% under CC-CV charging operation compared with the CC charging method and optimal conventional flow rate control method.

Key words: Vanadium redox flow battery, electrolyte flow rate, optimisation, energy saving, system efficiency, battery modelling.

*Corresponding Author

Email address: hao.wang05@adelaide.edu.au

Nomenclature		R_s	Overall stack resistance (Ω)
		Re	Reynolds number
ΔP	Pressure drop (Pa)	S	Active area (dm ²)
η_a	Activation overpotential (V)	SOC	State of charge
η_{con}	Concentration overpotential (V)	T	Temperature (K)
η_c	Charging energy efficiency	t	Time (s)
η_p	Pump efficiency	U	Volume (L)
η_s	System efficiency	V	Voltage (V)
К	Electrode porosity	W	Width (dm)
λ_{KC}	Kozenye-Carman constant	z	Number of electrons involved in the redox
μ	Electrolyte dynamic viscosity (Pa · s)	C-1	reactions
ho	Electrolyte density (kg \cdot m ⁻³)	Subscri	
ε	Permeability of electrode (dm ²)	a	Activation overpotentials
A	Cross section area (dm ²)	b	Battery
c	Concentration (mol \cdot L ⁻¹)	C	Charge
D	Thickness of membrane (dm)	ch	Inlet and outlet channels
d	Diameter (dm)	con	Concentration overpotentials
$E^{0'}$	Formal potential (V)	d	Discharge
E^0	Standard cell potential (V)	e	Electrode
F	Faraday's constant ($C \cdot mol^{-1}$)	f	Final
f	Minor loss coefficient	N	Negative side
FF	Flow factor	P	Positive side
H	Height (dm)	p	Pump
I	Current (A)	pp	Main pipes and manifolds V^{2+}
i	Current density (A · cm ⁻²)	2	V ³⁺
k	Diffusion coefficient ($m^2 \cdot s^{-1}$)	3	VO^{2+}
k_m	Mass transfer coefficient (dm \cdot s ⁻¹)	4	
L	Length (dm)	5	VO_2^+
N	Number of cells	Superso	•
P	Power (W)	OCV	Open circuit voltage
Q	Electrolyte flow rate (L/s)	S	Stack
R	Gas constant $(J \cdot mol^{-1} \cdot K^{-1})$	t	Tank
r	Cell ohmic resistivity $(\Omega \cdot cm^2)$	+	Positive half-cell
$r^{'}$	Overall cell resistivity $(\Omega \cdot cm^2)$	-	Negative half-cell
)	

1. INTRODUCTION

It is of general interest to integrate more renewable energy resources, such as wind and solar photovoltaic (PV), into the electricity generation mix. However, it can only be achieved by compensating for the unpredictable fluctuations and intermittency of these resources. As a result, energy storage systems (ESSs) are needed for technically and economically viable solutions. Among the different types of ESSs, Vanadium redox flow battery (VRFB) is one of the most promising solutions to tackle the technical challenges of intermittent sources due to its scalability, long lifespan, low maintenance cost and large storage capacity. In particular, the promising attributes of VRFB have drawn much attention from industry and academia to use the technology in microgrids and renewable energy (RE) power plants [1]. One major obstacle, however, is the low round-trip efficiency of VRFBs compared to other battery technologies, such as lithium-ions. Furthermore, the electrolyte temperature and flow rate significantly affect the performance and lifespan of VRFBs. Besides, a VRFB, as a typical flow battery, has two pumps to circulate electrolytes within each half-cell and tank, as shown in Fig. 1. This will impose unique operational challenges that are different from other battery types because the flow rate supplied by the two pumps will considerably affect the active species concentration in the tanks and stack, concentration overpotential, and pump energy consumption. As a result, the electrolyte flow rate is a decisive factor in the VRFB's efficiency. Thus, an appropriate electrolyte flow rate controller is vital to ensure the high performance of the VRFBs in the long term. In addition, the VRFB electrolyte flow rate determines the extent to which the battery system can be charged/discharged to both a high and low state of charge (SOC), thereby increasing the battery system's capacity utilization. This happens because the electrolyte flow rate supplies active species, which maintains the electrode surface concentration level at the end of the battery charging/discharging process.

The unique characteristics of electrolyte flow rate and its impact on the performance of VRFBs have been studied in the literature. Higher voltage efficiency can be achieved simply by increasing the flow rate, which reduces the concentration overpotential losses. However, in [2], a study on the flow rate considering pressure drop and concentration overpotentials showed that a higher flow rate leads to higher pump losses, thus decreasing the system efficiency. The results in [2] reveal that an optimised flow rate better minimises the total energy losses resulting in lower concentration overpotentials and pump energy consumption. In [3], an improved electrolyte flow rate control strategy is proposed to optimise the system efficiency throughout a charge and discharge cycle. The study results showed that battery capacity and system efficiency are optimised with the proposed strategy compared with a constant flow rate control method. A similar study has been carried out in [4] to obtain an optimised flow rate under different SOC levels, which had an interval of 10%. The drawback was discretizing the solution space at large intervals, which may result in a sub-optimal solution, hence, a lower system efficiency. The three studies, as mentioned earlier, highlighted that dynamically controlling the flow rate improves the overall efficiency of the VRFB system.

Instead of a constant flow rate, the concept of a variable flow rate, called conventional variable flow rate hereafter, has been developed based on Faraday's law of electrolysis. Faraday's first law of electrolysis was proposed based on the fact that the number of electrons passing through the electrolyte is proportional to the amount of chemical reaction on the electrodes during the electrolysis process. Based on this universal law, a variable flow rate controller, including SOC, current and a flow factor, is proposed to dynamically regulate the flow rate by using the proportional relationship between the chemical reaction and quantity of electrons. In [2], Tang et al. presented another flow rate optimisation method to gain high system efficiency performance

by finding the optimal flow rate among the conventional variable flow rate control method and constant flow rate control method. They concluded from the simulation result that conventional variable flow rates are superior to constant flow rates for a 40-cell VRFB system. A recent study by Karrech et al. in [5] suggests operating the VRFB by conventional variable flow rate results in higher capacity and energy efficiency. Since most of the commercial and experimental VRFB systems cannot implement variable flow rate control in practice due to the design of the pumps, they can only achieve a constant flow rate during the operation. An experimental validation in [5] compared these two conventional flow rate methods in system efficiency and capacity to validate efficiency gain in real-world operation.

Although the conventional variable flow rate has been recognised as an optimal solution for flow rate control to achieve higher capacity and system efficiency gain, it does not take the pump power consumption and other losses into account, which may limit the system performance by increasing the overall system losses for VRFB systems. Moreover, the conventional variable flow rate is determined by the SOC and current during the operation, neglecting the active species imbalance in the VRFB system between the stack to the two electrolyte storage tanks. As a result, it may degrade the battery capacity and system efficiency of the VRFB system. To manage the above-mentioned drawbacks in flow rate optimisation, model-based optimisation methods are proposed and investigated to find the optimal flow rate during normal operation at high-resolution intervals. Based on accurate VRFB multi-physics and pump models, the active species in the stack/tanks and pump energy consumption can be accurately estimated to form a dynamic optimisation process. In [6], a model-based optimisation method is proposed to determine the optimal flow rate to maximise the system efficiency. The simulation results show that this innovative approach contributes to an efficiency gain of up to 1.2%, with a capacity gain of up to 5.4%. The caveat is that the proposed point-based optimisation method may not be able to optimise the flow rate under a variable charging regime due to the rapid fluctuations in the battery voltage, SOC, and current parameters. Two optimal charging case studies for VRFB are presented in [7, 8] to obtain an optimised electrolyte flow rate during the battery charging process. The model-based nonlinear optimisation approach in [7, 8] has shown several advantages in loss reduction and energy efficiency improvement. However, the flow rate optimisation during discharging has not been investigated to show the system efficiency improvement throughout a full charging/discharging cycle.

In a recent study presented in [9], another optimal flow rate strategy is proposed to enhance the system efficiency compared with constant and conventional variable flow rate control methods. Similar to other studies, the proposed method is only evaluated under CC charging/discharging. While the proposed strategy shows a 0.17% improvement in the system efficiency under voltage limits from 1.1 to 1.7V, it performs worse regarding the depth of discharge (DOD) by 3.5% compared with the conventional variable flow rate. Another dynamic flow rate strategy was introduced in [10] to optimise the flow rate under a variable power profile by explicitly assessing the effect of thermal dynamics. The results showed that the proposed strategy yields a small improvement in stack efficiency, system efficiency and concentration overpotential losses compared to the conventional variable flow rate method. In [11], an optimal charging current and flow management scheme is developed to achieve fast charging at high energy efficiency. However, the energy-saving performance of the proposed flow management scheme has not been compared with the results of the conventional variable flow rate method to validate its efficiency gain.

This paper presents a dynamic nonlinear optimisation method to derive the optimal flow rate by maximising system efficiency. This study is conducted as a simulation study based on a validated multi-physics VRFB model, where the energy saving under the proposed optimisation method is analysed comprehensively. The main contributions of this paper are as follows:

- Most studies, e.g., [2, 3, 4, 6, 7, 8, 10, 11], evaluated their proposed optimisation methods using a VRFB model that was not validated by experimental data; hence, the model accuracy is unknown. This study validates the VRFB model based on experimental data for a 5kW/3kWh laboratory-scale VRFB system with actual manufacturing configurations.
- In most studies, e.g., [2, 3, 4, 6, 9], the CC charging method is used to investigate the feasibility of the proposed optimisation methods under a varying power regime, which may not be practical. In this study, a varying power profile is used to evaluate the performance of the proposed flow rate optimisation method.
- Case studies in CC and CC-CV charging regimes with 40A, 60A, 80A and 100A charging/discharging currents are carried out to show the robustness of the proposed flow rate optimisation method in achieving a higher system efficiency gain across the board compared to the conventional variable flow rate control method. Meanwhile, the energy-saving capability of the CC-CV method is thoroughly assessed and verified for high-current charging applications.
- In-depth analyses are carried out to investigate the performance of the proposed method in loss reduction. Also, the performance of the CC and CC-CV charging regimes in reducing active species imbalance is investigated to demonstrate the necessity of using the CC-CV charging method in reducing capacity fading.
- A simplified 2D lookup table is constructed from the simulation results obtained by the
 proposed optimisation-based method that is beneficial as an online flow rate controller. It
 has been validated considering the system degradation caused by active species imbalance
 over 100 cycles.

The structure of this paper is organised as follows: in Section 2, a comprehensive multiphysics VRFB model is presented with detailed battery configurations. Section 3 introduces the proposed model-based nonlinear dynamic optimisation (MNDO) method, while the comprehensive VRFB multi-physics model is validated in Section 4. Three case studies are carried out in Section 4 to validate the effectiveness of the proposed MNDO in energy-saving and highlight the benefits of using a two-stage charging method. Finally, in-depth discussions are given in Section 5 to conclude the significance of the flow rate control in system efficiency gain. More importantly, an efficient online flow rate optimisation method using a 2D lookup table is proposed from the offline MNDO results that can achieve high performance without requiring high computational resources. Also, further discussion on the loss reduction of VRFB systems by flow rate control and the performance of different charging methods in capacity fading is presented in Section 5.

2. VRFB Model development

The VRFB normally consists of two electrolyte tanks, pumps and a stack to form a complete system, as shown in Fig. 1. These main components facilitate electrolyte circulation across each half-cell and tank, which uses vanadium redox couples during charging and discharging.

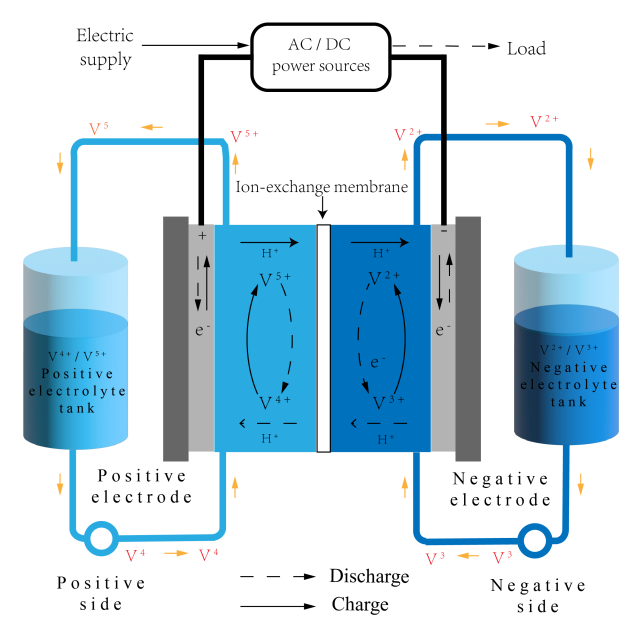


Figure 1: A schematic diagram of a typical VRFB system [1]

During the charging process, the battery is connected to a power source, and the oxidation of VO_2^+ in the positive half-cell and deoxidation of the V_3^+ in the negative half-cell occur due to the input current with the movement of the ions from the electrode to the electrolyte. During the discharging process, the reverse chemical reactions take place, where electrons are generated and collected by the current collector. The negative/positive half-cell reactions and overall cell reactions can be shown as follow:

Negative half-cell reactions:

$$V^{3+} + e^- \stackrel{\text{Charge}}{\rightleftharpoons}_{\text{Discharge}} V^{2+} \quad E_N^0 = -0.255 V$$
 (1)

Positive half-cell reactions:

$$VO^{2+} + H_2O \underset{\text{Discharge}}{\rightleftharpoons} VO_2^+ + 2H^+ + e^- \quad E_P^0 = 1.004V$$
 (2)

Overall cell reactions:

$$VO^{2+} + V^{3+} + H_2O \underset{\text{Discharge}}{\overset{\text{Charge}}{\rightleftharpoons}} VO_2^+ + V^{2+} + 2H^+$$
 (3)

To investigate the flow rate optimisation, a dynamic multi-physics model is implemented based on VRFB modelling work done by Tang et al. in [12]. Several assumptions, as presented below, are made to reduce the complexity of the optimisation problem:

• The VRFB charging/discharging cycles are carried out at the constant ambient temperature of 25°C, and the electrolyte temperature in the stack is assumed constant which is the same as the ambient temperature [11].

- The electrolytes in the tanks and stack are fully balanced before the battery operation, and the total electrolyte volume in this VRFB system remains constant.
- The stack is well designed; thus, the shunt current loss can be neglected [13]. Also, hydrogen evolution and other gasses are not considered.
- Due to the manufacturing limitations, the configuration of the membrane is unknown. In this study, the membrane is assumed to be Nafion 115, and the diffusion coefficients of vanadium species and the thickness of the membrane are obtained from [6].
- The overall cell resistivity remains constant over the operating SOC from 15% to 85%.
- Oxidation of vanadium species is not considered in this study [14].
- Self-discharge reactions from the cross-over phenomenon are instantaneous [14].

2.1. Dynamic multi-physics model

The dynamic model used in the optimisation algorithm is derived from the conservation of mass and energy balance equations. In particular, the core of the multi-physics model is based on molar conservation equations to simulate the variations in active species concentrations due to the current and ion diffusion across the membrane. The multi-physics model describes the relationships between the flow rate and the SOC, stack voltage and vanadium ion concentrations, which are necessary to show the impact of the flow rate on the VRFB performance. Moreover, a hydraulic model of the pump is established within the dynamic model to estimate its energy consumption during the operation.

2.1.1. Mass balance for vanadium ions

The mass balance for vanadium ions quantifies the transfer of vanadium ions through the membrane, and is formulated based on Fick's law. In [12], the mass balance in the pipes is neglected, but the membrane diffusion coefficient is considered to be affected by the stack temperature. To reduce the complexity of the optimisation algorithm, this study assumed the stack temperature is constant, hence, the effect of the electrolyte temperature on the membrane can be neglected. The mass balance model for vanadium ions is established based on the law of conservation of mass, that is, the total mass of vanadium ions is constant throughout its lifespan.

For vanadium ions in the stack:

$$\frac{U_{stack}}{2} \frac{dc_2^s}{dt} = Q\left(c_2^t - c_2^s\right) \pm \frac{NI}{zF} - Nk_2 \frac{c_2^s}{D} S - 2Nk_5 \frac{c_5^s}{D} S - Nk_4 \frac{c_4^s}{D} S$$
(4)

$$\frac{U_{stack}}{2} \frac{dc_3^s}{dt} = Q\left(c_3^t - c_3^s\right) \mp \frac{NI}{zF} - Nk_3 \frac{c_3^s}{D} S
+ 3Nk_5 \frac{c_5^s}{D} S + 2Nk_4 \frac{c_4^s}{D} S$$
(5)

$$\frac{U_{stack}}{2} \frac{dc_4^s}{dt} = Q\left(c_4^t - c_4^s\right) \mp \frac{NI}{zF} - Nk_4 \frac{c_4^s}{D} S
+ 3Nk_2 \frac{c_2^s}{D} S + 2Nk_3 \frac{c_3^s}{D} S$$
(6)

$$\frac{U_{\text{stack}}}{2} \frac{dc_5^s}{dt} = Q\left(c_5^t - c_5^s\right) \pm \frac{NI}{zF} - Nk_5 \frac{c_5^s}{D} S - 2Nk_2 \frac{c_2^s}{D} S - Nk_3 \frac{c_3^s}{D} S$$
(7)

For vanadium ions in the tanks:

$$U_N \frac{dc_2^t}{dt} = Q\left(c_2^s - c_2^t\right) \tag{8}$$

$$U_N \frac{dc_3^t}{dt} = Q\left(c_3^s - c_3^t\right) \tag{9}$$

$$U_P \frac{dc_4^t}{dt} = Q\left(c_4^s - c_4^t\right) \tag{10}$$

$$U_P \frac{dc_5^t}{dt} = Q\left(c_5^s - c_5^t\right) \tag{11}$$

The positive/negative tank, pipe and each positive/negative half-cell form an electrolyte circulation path to supply vanadium ions for reactions during charging and discharging. As a result, the flow rate, as the factor linking the vanadium ion concentrations in the tanks and stack, plays a vital role in the operation and performance of the VRFB.

2.1.2. Multi-physics model

The multi-physics model links the chemical dynamic with the electrical performance and parameters of VRFB, including open-circuit voltage (OCV), overpotentials and stack voltage etc. The OCV is defined as the voltage of the electrochemical cell without current flow in or out, also defined as the potential difference across the positive and negative electrode, shown in Eq. (12) from [9] and derived by the Nernst equation.

$$E^{OCV} = E_p - E_n = E^0 + \frac{RT}{zF} \ln \left(\frac{C_{V^{2+}} C_{VO_2^+} C_{H^+}^2}{C_{V^{3+}} C_{VO^{2+}}} \right); E^0 = 1.26 \text{V}$$
 (12)

In the OCV equation in Eq. (12), C_{H^+} represents the hydrogen ion concentrations. To simplify the equation, assuming this term remains constant, the standard cell potential E^0 can be expressed alternatively as a new formal potential term E^{0} by experimentally measuring the open circuit potential when the SOC is at 50%. This value is reported as $E^{0'} = 1.4V$ in [15].

$$E^{OCV} = E^{0'} + \frac{RT}{zF} \ln \left(\frac{C_{V^2 +} C_{VO_2^+}}{C_{V^3 +} C_{VO_2^{2+}}} \right); E^{0'} = 1.40V$$
 (13)

The activation overpotential, concentration overpotential and ohmic overpotential, and OCV sum to form the battery terminal voltage. Since the activation overpotential is negligible and independent of the flow rate, normally, the ohmic resistance and the activation overpotentials are combined and expressed by an overall ohmic voltage drop [14], as shown in Eq. (14). In this equation, r represents the ohmic resistance, r' represents the overall cell resistivity with the activation overpotential η_a , and i and r stand for the current density and area-specific resistance.

$$i \cdot r' = i \cdot r + \eta_a^+ + \eta_a^- \tag{14}$$

The concentration overpotential affects the cell voltage at different SOC levels during charging and discharging, which is caused by the mass transfer of reactants from the bulk electrolyte to the electrode surface [14]. In [2], Tang et al. expressed the concentration overpotential using the Nernst equation and Fick's law. Later, Yifeng in [13] demonstrated the expression of the concentration overpotential based on Tang's results and specified the equations of concentration overpotential during charging and discharging, which are:

$$\eta_{con}^{+} = \begin{cases} -\frac{RT}{zF} \ln(1 - \frac{I}{nFk_m L_e H_e c_4}), & \text{charging} \\ -\frac{RT}{zF} \ln(1 - \frac{I}{nFk_m L_e H_e c_5}), & \text{discharging} \end{cases}$$
(15)

$$\eta_{con}^{-} = \begin{cases}
-\frac{RT}{zF} \ln(1 - \frac{I}{nFk_{m}L_{e}H_{e}c_{3}}), & \text{charging} \\
-\frac{RT}{zF} \ln(1 - \frac{I}{nFk_{m}L_{e}H_{e}c_{3}}), & \text{discharging}
\end{cases}$$
(16)

In Eqs. (15)-(16), L_e and H_e are the length and height of the electrode, k_m is the mass transfer coefficient and can be approximated by Eq. (17) from [7], and W_e and Q_{cell} represent the width of the electrode and the flow rate for each cell, respectively.

$$k_m = 1.6 \times 10^{-3} \left(\frac{Q_{cell}}{10L_e W_e} \right)^{0.4} \tag{17}$$

In this multi-physics model, the stack voltage is obtained from the Nernst equation with OCV, ohmic overpotential and concentration overpotential expressed in Eq. (18), where N is the number of cells.

$$V_{\text{stack}} = N(E^{OCV} + ir' + \eta_{con}^+ + \eta_{con}^-)$$
(18)

The vanadium ion concentrations determines the SOC of the VRFB system in the negative and positive tanks by taking the average value of the SOC in the two tanks.

$$SOC_N = \frac{c_{V^{2+}}}{c_{V^{2+}} + c_{V^{3+}}} \tag{19}$$

$$SOC_P = \frac{c_{VO_2^+}}{c_{VO_2^+} + c_{VO^{2+}}} \tag{20}$$

$$SOC = \frac{SOC_N + SOC_P}{2} \tag{21}$$

Table 1 summarises all the parameters and their definitions used in this study.

2.1.3. Hydraulic system model

The pump consumes energy during VRFB operation to circulate electrolytes between the tanks and stacks. The pump energy consumption has a significant impact on the overall system efficiency. Therefore, there is a trade-off between the pump energy losses and the overall system's efficiency with an obvious impact on the VRFB's overall performance. To write the objective functions for optimal VRFB operation and determine the system efficiency, we adopted a hydraulic system model from [13] to calculate the pressure drop in the hydraulic system. It contains three pressure drops, including the pressure drop in the main pipes and manifolds, as

Table 1: VRFB model parameters and definition in this study

Symbol	Definition	Value
N	Number of cells in the stack	37
С	Total concentration of vanadium ions in mol/L	1.5
U_N	Volume of the electrolyte in negative tank in L	70
U_P	Volume of the electrolyte in positive tank in L	70
U_{stack}	Volume of the stack in L	40
H_e	Height of the electrode in dm	3
L_e	Length of the electrode in dm	7
W_e	Width of the electrode in dm	0.025
S	Active area in dm ²	21
d	Thickness of the membrane in dm	$1.27e^{-3}$
T	Ambient temperature in K	298.15
R	Gas constant in Jmol ⁻¹ K ⁻¹	8.314
$\overline{\rho}$	Electrolyte density in kg m ⁻³	1300
\overline{F}	Faraday's constant in C ⋅ mol ⁻¹	96,485
r'	Overall cell resistivity in $\Omega \cdot \text{cm}^2$	2.72
k_2	Diffusion coefficient of V^{2+} in m^2s^{-1}	$8.768e^{-12}$
k ₃	Diffusion coefficient of V^{3+} in m ² s ⁻¹	$3.222e^{-12}$
k_4	Diffusion coefficient of V^{4+} in m ² s ⁻¹	$6.825e^{-12}$
k ₅	Diffusion coefficient of V^{5+} in m^2s^{-1}	$5.897e^{-12}$

in Eq. (22), the pressure drop from the channel, as in Eq. (23), and the pressure drop from the porous electrode, given in Eq. (24):

$$\Delta P_{pp} = \frac{64}{\text{Re}} \frac{L_{pp}}{d_{pp}} \frac{\rho Q^2}{2A_{pp}^2} + f \frac{\rho Q^2}{2A_{pp}^2}$$
 (22)

$$\Delta P_{ch} = \frac{64}{\text{Re}} \frac{L_{ch}}{d_{ch}} \frac{\rho\left(\frac{Q}{N}\right)^2}{2A_{ch}^2} + f \frac{\rho\left(\frac{Q}{N}\right)^2}{2A_{ch}^2}$$
(23)

$$\Delta P_e = \frac{\mu H_e \left(\frac{Q}{N}\right)}{\kappa L_e W_e} \tag{24}$$

where Re is the Reynolds number expressed as in (25), and κ is the permeability of the porous electrode and expressed as in (26):

$$Re = \frac{\rho d_{pp}Q}{\mu A_{pp}} \tag{25}$$

$$\kappa = \frac{d_f^2}{16\lambda_{KC}} \frac{\varepsilon^3}{(1-\varepsilon)^2}$$
 (26)

The configurations of the main pipe, the channel, and the porous electrode are summarised in Tables 2, respectively, which are used for the simulation studies in this paper. Note that the electrode dimensions are also given in Table 2.

The total pressure drop of the hydraulic system is then expressed as the sum of the pressure drops from the main pipe, channel and electrode:

$$\Delta P_{total} = \Delta P_{pp} + \Delta P_{ch} + \Delta P_e$$

$$10$$
(27)

Table 2: Configurations of the main pipe, channel and porous electrode

Symbol	Definition	Value
L_{pp}	Length of the pipe in dm	20
d_{pp}	Inner diameter of the pipe in dm	0.13
ρ	Electrolyte density in g cm ⁻³	1.354
A_{pp}	Cross section area of pipes in dm ²	0.013
μ	Electrolyte dynamic viscosity in Pa·s	$4.928e^{-3}$
\overline{f}	Minor loss coefficient	0.9
L_{ch}	Length of the channel in dm	7
d_{ch}	Diameter of the channel in dm	0.03
A_{ch}	Cross section area of channel in dm ²	$7e^{-4}$
d_f	Fibre diameter of the channel in dm	$1.76e^{-4}$
ε	Electrode porosity	0.93
λ_{KC}	Kozenye-Carman constant	4.28

The total pump power losses in these two pumps can be expressed as:

$$P_p = 2 \cdot \frac{\Delta P_{total} \cdot Q}{\eta_p} \tag{28}$$

This study adopts a typical variable speed pump efficiency curve from [7]. The pump efficiency varies from 30% to 70% with the flow rate changing from 0.05L/s to 1.26L/s, which is used to simulate the overall efficiency variations of a normal variable speed pump [7].

2.2. Conventional flow rate control

Constant and conventional variable flow rates are two conventional flow rate control strategies used to control the pump speed for the electrolyte circulation during operational cycles. The constant flow rate strategy operates the pumps at a fixed level for supplementing hydrogen ions and active species. In contrast, the conventional variable flow rate method is derived from Faraday's law of electrolysis mentioned in the introduction. The conventional variable flow rate is determined by Eqs. (29)-(30) during the charging and discharging process, where N is the number of cells in the stack, FF is the flow factor representing the conversion per pass [13], and c is the overall electrolyte vanadium concentration.

The conventional variable flow rate has been studied and identified as an improved flow rate control method to yield higher capacity and efficiency both in simulations and experiments [2, 4, 5]. The variable flow rate method utilises a lower flow rate at the initial stage of charging/discharging when the actives species in the stack are sufficient, and this contributes to saving pump energy losses compared with constant flow rate. As the charging/discharging process reaches higher/lower SOC levels, the variable flow rate is raised to supply active species to the stack from the tanks, maintaining the bulk concentration level to charge/discharge the VRFB higher. These characteristics of the conventional variable flow rate control method demonstrate its advantages over the constant flow rate control by balancing the concentration overpotential and pump power losses to maintain a higher efficiency. As a result, in this study, the conventional variable flow rate control method with various stoichiometry flow factors is used as the base case to evaluate the performance improvements of the proposed MNDO method. The conventional variable flow rate derivation is given in Eqs. (29)-(30). This paper proposes a variable flow rate method with an optimal FF that achieves the highest system efficiency which is referred to as optimal conventional flow rate (CFR) control.

$$Q = N \cdot FF \cdot \frac{|I|}{nEc(1-SOC)}, \quad \text{charging}$$
 (29)

$$Q = N \cdot FF \cdot \frac{|I|}{nFc(SOC)},$$
 discharging (30)

Finally, to evaluate the performance of the proposed MNDO method in energy-saving compared with the optimal CFR method, a system efficiency derivation is introduced as [2]:

$$\eta_s = \frac{\int_{t_0}^{t_f} P_c - 2P_p dt}{\int_{t_0}^{t_f} P_d + 2P_p dt}$$
 (31)

where t_0 and t_f stand for the initial time and end time for the charging/discharging process, and P_c and P_d are the charging/discharging power of the VRFB system, while $2P_p$ is the total power consumption during charging/discharging process.

3. The proposed optimised flow rate strategy

The electrolyte flow rate significantly affects the system-level efficiency and capacity of VRFBs by affecting the total pump power consumption, concentration overpotential and active species level in the stack. To enhance the system efficiency of VRFBs, an optimal electrolyte flow rate can be used to balance the losses during the battery operation as mentioned in [2]. Considering the problem mentioned above, a model-based dynamic optimisation method is proposed in this paper. The flow rate is optimised considering two objective functions during the charging and discharging process. The two cost functions aim to find the optimal flow rate that minimises the total charging energy and maximises the total discharging energy during full or partial charging/discharging cycles are defined as:

Cost function (Objective function):

$$\min_{Q(t)} J = \int_{t_0}^{t_f} \left(IV_{stack} + P_p \right) dt \quad \text{charging}$$

$$\max_{Q(t)} J = \int_{t_0}^{t_f} \left(IV_{stack} - P_p \right) dt \quad \text{discharging}$$
with an experience. (32)

with constraints:

$$Q_{min} \le Q \le Q_{max}$$
 $SOC_{min} \le SOC \le SOC_{max}$

The constraints are basic linear physical constraints on the pump flow rate (i.e., 0.1L/s to 0.8L/s) and SOC range (i.e., 15% to 85%) to prevent the VRFB system from being overcharged or over-discharged.

In the two cost functions, the stack voltage is a nonlinear function that contains the flow rate to derive the concentration overpotential using Eqs. (15)- (17). Thus, this model-based dynamic optimisation problem is a nonlinear optimisation called model-based nonlinear dynamic optimisation (MNDO). To optimise the flow rate based on the cost functions, considering the variations of VRFB systems in stack voltage, current and other states, an iterative optimisation process is necessary to dynamically find the optimal flow rate within a small time interval. Taking all these considerations into account, a proposed MNDO method is developed, and its principle is shown in Fig. 2. The proposed MNDO method is solved every 1s starting from t_0 to t_f . Furthermore, an efficient constrained trust region optimisation method is necessary to find the local

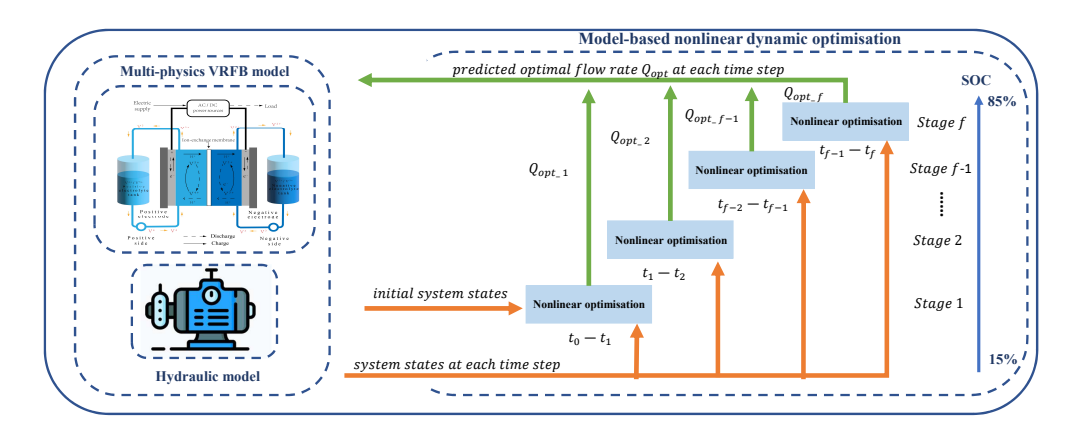


Figure 2: Flow chart of this proposed MNDO method

Algorithm 1 Sequential quadratic programming (SQP) implementation

- 1: Initialization: Define a possible initial searching point; set the objective function convergence tolerance and iteration stop criteria (lower than 1e-6 or after 50 iterations)
- 2: repeat
- 3: Update Hessian matrix *H* by quasi-Newton method
- 4: Solve the quadratic programming problem with constraints, *d* is the trial step:

$$\min_{d \in \mathfrak{R}^n} q(d) = \frac{1}{2} d^T H d + c^T d$$

- 5: Update new trial step *d* for next iteration
- 6: until the objective function tolerance is lower than 1e-6 or after 50 iterations

Output: optimal flow rate Q_{opt-k} at each time step T = k

minimum value of the objective function in this study. The sequential quadratic programming (SQP) algorithm is an iterative constrained nonlinear optimisation method that is effective for cost function-based optimisation problems. The principle of the SQP algorithm is to find the local minimum of the cost function while satisfying the constraints; it is one of the trust region optimisation methods. The SQP algorithm finds a possible initial point and next updates the Hessian matrix to generate a simpler function to approach the local minimum. The SQP algorithm realises the adaptive trail step in each iteration and stops when the tolerance reaches the pre-set value or the iteration number reaches the maximum number. The SQP is efficient for 1-D searching problems with simple constraints, which shows good performance in convergence, boundary searching capability and computational efficiency. To find the optimal flow rate at each time step, the SQP algorithm is adapted here and is used to solve the developed multi-physics VRFB model. The optimisation process here drew on the principle of the model predictive control (MPC) problem, which predicts the system dynamics based on the information in the current time step and searches for the optimal flow rate in the next time step. The pseudocode for the optimisation problem implementation is given in Algorithm 1.

4. Case studies and results

In Section 2, a multi-physics VRFB model was presented to investigate the dynamic characteristics and performance of a laboratory-scale VRFB system with a specific configuration. Based on the proposed battery model, the performance of the conventional flow rate approaches is evaluated to be used as base cases for comparison purposes. In this section, first, the system configurations and operational conditions are presented. Second, the VRFB model is validated using experimental data to show its accuracy. Then, CC and CC-CV charging methods are introduced. Finally, simulation studies are carried out for three case studies to quantify the performance of the proposed dynamic optimisation method in comparison to the conventional methods under a dynamic power operation scenario. The differences between CC and CC-CV charging methods are highlighted in this subsection.

4.1. System configurations and operational conditions

A 5 kW/3 kWh experimental VRFB system is considered in this case study that contains 37 cells with an ion-exchange membrane, bipolar plates, current collectors, flow channels, porous electrodes, end plates, electrolyte tanks and pumps. Each electrolyte tank has a capacity of 70L, hence the total electrolyte volume is 140L. Also, the total vanadium concentration is 1.5mol/L.

The VRFB system was tested with a constant charge/discharge current at 60A, 80A and 100A, with a terminal voltage range from 40V-60V under an ambient temperature of 25 °C in the lab. The experiments are carried out with a constant flow rate at 1m³/h using the two peristaltic pumps for electrolyte circulation, and the initial SOC of this VRFB system is 10%.

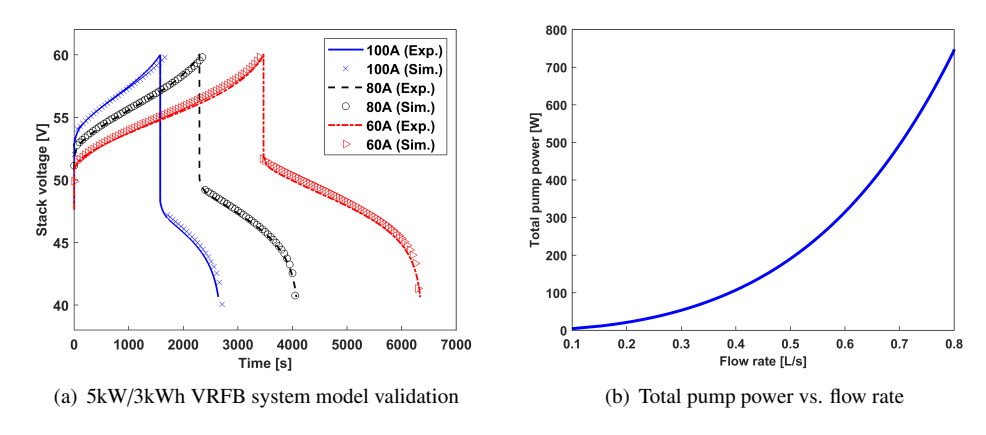


Figure 3: Developed multi-physics model validation and hydraulic model result

4.2. Model validation

The dynamic multi-physics model with hydraulic system model introduced in Section 2 is built in Matlab/Simulink 2021a to simulate the performance of the VRFB system using the parameters in Tables 1-2. shows validation of the simulation results compared to the experimental results under 60A, 80A and 100A charging/discharging currents with a constant flow rate, as mentioned in the previous section. The mean absolute error of our proposed method under the three current regimes is 1.86%, which shows a better performance compared to the results in [9].

Due to the measurement of overpotentials being difficult to validate on an industrial-scale VRFB system and the pump used in this study being constant, the validation of overpotentials and pump power cannot be performed in this study, which is a common limitation in VRFB research. The model validation results follow the experimental results in the laboratory environment. In Fig. 3 (b), the total pump power vs. flow rate results are demonstrated with a lower flow rate range from 0.1 L/s-0.8 L/s, and the total pump power consumption varies between 10W to 750W based on the calculation.

4.3. Charging methods

To safely charge the battery to prevent overheating and overcharging issues, several charging approaches have been studied and developed, including constant current (CC), constant voltage (CV) and constant current- constant voltage (CC-CV) methods. The CC mode is the most straightforward method of charging the battery with a constant current. The merits of the CC method include easy calculation of the charging time and SOC of the battery system. Nevertheless, the stack voltage and temperature in this approach may exceed safe limits after a long charging period, which may lead to overcharging and eventually cause damage by gas evolution and thermal precipitation for VRFBs. A suitable SOC range is vital for the CC method to terminate the charging process and prevent overcharging.

The CV method is involved applying by connecting a constant voltage source to the battery's terminals. At the initial stage of the charging process, the charging current remains constant and it reduces during charging until reaches a pre-set limit. However, the CV charging method without safe current limits at the early charging stage may lead to high heat generation inside the battery stack, damaging the battery stack and degrading the battery lifespan. To overcome the shortcomings of the CV and CC method, a two-step method called the CC-CV method is proposed which uses the CC method at the initial stage of the charging process until the battery voltage reaches a given limit. At that point, the CV method is applied which maintains the battery voltage at a pre-defined limit to prevent overcharging. The CC-CV method combines the benefits of CC and CV, and is considered the most efficient and commonly used method for safe battery charging [16].

Due to the variations of charging current in the CC-CV charging mode, a recursive function is proposed in [17] to update the current in CV mode as follows:

$$I(k) = I(k-1) - N \left[E^{OCV}(k) - E^{OCV}(k-1) + \eta_{con}(k) - \eta_{con}(k-1) \right] / R_s$$
 (33)

where N is the number of cells, $E^{OCV}(k)$ is the OCV of a single cell at time k, $\eta_{con}(k)$ is the concentration overpotentials of a single cell at time k, and R_s is overall resistance of the VRFB stack in the charging mode. Updating the current in Eq. (33) maintains the stack voltage level at the pre-defined limit as in the CV charging method.

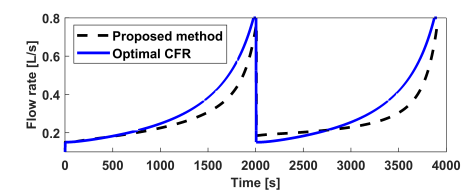
4.4. Case study 1: Dynamic model-based optimisation of electrolyte flow rate under a hypothetical charging/discharging cycle by constant current

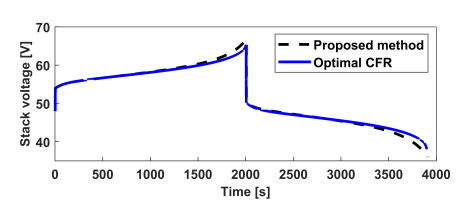
The energy-related performance of the optimal flow rate derived from the proposed method and the optimal CFR method under different constant charging/discharging currents is given in Table 3. This contains a detailed comparison of system efficiency, capacity, total energy consumption for charging and system efficiency gain obtained by the proposed method for a complete charging-discharging cycle. During the simulation study, the VRFB system was fully

charged from 15% to 85% SOC and fully discharged to 15% SOC at different constant charging/discharging currents (60A, 80A and 100A) to represent a hypothetical charging/discharging cycle. With the increased charging/discharging current from 60A to 100A, the system efficiency reduced by 5% for both flow rate control methods. The increased charging/discharging current caused overpotential losses, and the pump energy consumption rose significantly. By comparing the system efficiency obtained from the proposed MNDO method versus the optimal CFR control method with a flow factor of 5 and 4, an efficiency gain of up to 0.33% at 80A current is achieved. The lowest efficiency gain of 0.14% is achieved at 100A charging/discharging current.

Table 3: Results of optimal CFR and FR in the CC charging mode

	Conventional flow rate control method			Proposed optimal flow rate control method		
Current	FF	Capacity	System efficiency	Capacity	System efficiency	Efficiency gain
		(kWh)		(kWh)		
100A	5	2.33	70.58%	2.34	70.72%	0.14%
80A	5	2.40	73.59%	2.41	73.92%	0.33%
60A	4	2.45	75.69%	2.46	76.00%	0.31%





(a) Electrolyte flow rate obtained from the two methods

(b) Stack voltage profile obtained from the two methods

Figure 4: Simulation results of 100A constant charging/discharging current by the proposed method and optimal CFR with FF=5

Further simulation results, i.e., flow rate and stack voltage profiles, are shown in Fig. 4 under 100A charging/discharging current. In Fig. 4 (a), the optimal FR by the proposed method is compared with the one from CFR, and the stack voltage performance is compared in Fig. 4 (b). The main difference between these two flow rate curves is that the proposed method has a more gentle increase trend than the optimal CFR determined by Faraday's law of electrolysis. At the end of the charging/discharging process, both methods rise to a high flow rate level to avoid low bulk concentration, which prevents battery capacity reduction before it arrives at the voltage limits. As for the stack voltage performance, a lower electrolyte flow rate will increase the concentration overpotential, thus causing the small stack voltage rise during charging, as shown in Fig. 4 (b). This phenomenon becomes more significant at the late stage of the charging/discharging process because the active species in the VRFB stack drop to a lower concentration level. A more detailed analysis of the optimal flow rate derived by the proposed method in loss reduction and active species balance will be presented in Section 5 to demonstrate the underlying advantages of the proposed flow rate control method.

4.5. Case study 2: Dynamic model-based optimisation of electrolyte flow rate under CC-CV charging mode

In Section 4.3, the CC-CV charging method was introduced to efficiently utilise the charging energy and stabilise the battery temperature, which has been commonly applied in lithium-ion batteries and other solid-state batteries. To evaluate the performance of the CC-CV charging method in the VRFB compared to the CC charging method in charging energy reduction, a CC-CV charging method with a voltage limit of 60V in the CV charging period is adopted in this study. The battery has been charged from 15% to 85% SOC in this simulation study. Table 4 compares CC and CC-CV charging methods to highlight the energy-saving ability of the CC-CV charging mode. To do so, a charging energy efficiency equation is obtained from [7] for comparison in Eq. (34). Note that P_b^{ideal} is the ideal charging power that neglects the concentration overpotential and ohmic overpotential, and P_b is the overall charging power considering these two overpotentials. $2P_p$ is the two pumps' power consumption at each time step, t_0 and t_f stand for the initial and final charging time, respectively.

$$\eta_c = \frac{\int_{t_0}^{t_f} P_b^{ideal} dt}{\int_{t_0}^{t_f} P_b + 2P_p dt}$$
 (34)

An energy-related performance and charging time comparison for the proposed MNDO method under CC and CC-CV charging methods are shown in Table 4. The efficiency gain in this table is obtained by comparing the charging energy efficiency between these two charging methods. It can be seen that charging energy efficiency can increase up to 1.39% at 100A charging current, decreases under the CC approach, and has almost no improvement at the lowest charging current 60A. With CV mode being used in the charging process, a reduction in charging current is unavoidable during CV charging, which increases the charging time and the pump energy consumption. In high-current charging applications, the excessive charging time can be seen as a result of the early arrival of the CV charging mode, which in turn leads to a greater reduction in charging current in each time step. These results underline the benefits of using the CC-CV method in high-current charging applications without considering fast-charging issues. Nevertheless, in the low current charging applications, due to the low concentration of overpotential losses and late arrival to the pre-set limits, the CC-CV charging method does not offer superior performance in loss reduction. It even causes more pump energy consumption due to increased charging time.

Table 4: Comparison results of optimal flow rate under CC and CC-CV charging modes

	Proposed optimal flow rate control method			Charging time comparison		
Current	Charging energy efficiency of CC	Charging energy efficiency of CC-CV	Charging efficiency gain	Charging time under CC mode	Charging time under CC-CV mode	Difference
100A	88.16%	89.55%	1.39%	2006s	2263s	257s
80A	90.44%	90.99%	0.55%	2533s	2674s	141s
60A	92.61%	92.73%	0.12%	3433s	3470s	35s

In Figs. 5 (a)-(d), an extensive comparison of current, SOC, stack voltage, and flow rate is shown with 100A current under CC-CV and CC modes obtained by the proposed MNDO method. The current profiles in Fig. 5 (a) illustrate the principle of CV charging mode, which leads to charging current variations. After the stack voltage reached the pre-set limit, a voltage source of 60V was applied to the VRFB system for CV charging; thus, the charging current was

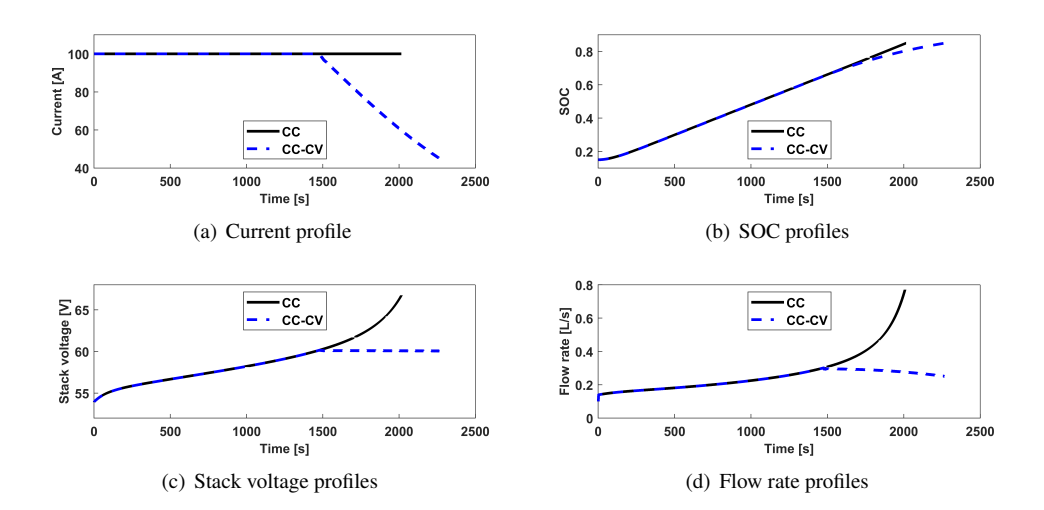


Figure 5: The performance of the proposed method under CC & CC-CV charging modes at 100A constant charging current and 60V constant voltage

decreased to reduce the ohmic and concentration overpotential to maintain the stack voltage level. However, decreasing the charging current required an additional 257s to charge the battery fully. The SOC profiles in Fig. 5 (b) demonstrate the drawback of CC-CV mode under fast-charging scenarios in which more time is needed for charging due to the decline of charging current.

The stack voltage performance under CC and CC-CV modes in Fig. 5 (c) shows the merits of the CC-CV approach in charging, resulting in a lower charging current applied to reduce the losses caused by concentration overpotential in CV charging period. However, the increase in charging time will inevitably lead to pump energy consumption due to the longer charging time. Further analysis of the loss reduction in the CC-CV charging mode will be presented in Section 5 to highlight the advantages of this charging approach in high-current charging applications.

Moreover, the derived optimal flow rate in the CC and CC-CV charging modes are shown in Fig. 5 (d). As the charging mode switches to CV, these two optimal flow rates exhibit different trends. This observation can be explained by looking at the downward trend of optimal flow rate in the CC-CV mode caused by the decline in charging current, helping to reduce the concentration overponential loss. Thus, a lower flow rate is more efficient to minimise the losses in concentration overpotential and pump energy consumption. Furthermore, the result in Fig. 5 (d) emphasizes another benefit of the CC-CV charging mode: a smaller pump can manage high-current charging applications and reach a high SOC level. For example, in this case, the maximum flow rate required to charge the VRFB system to 85% SOC level in the CC-CV charging mode is 0.3L/s. However, the same flow rate can only charge the VRFB system to 67% in the CC charging mode.

4.6. Case study 3: Dynamic model-based optimisation of electrolyte flow rate under varying power regime

Section 3 explained that the proposed MNDO method considers the dynamics of the VRFB system and searches for the optimal flow rate at each time step. This feature is ideal for handling varying power and current regimes to maximise the energy usage of the VRFB system. Here, a

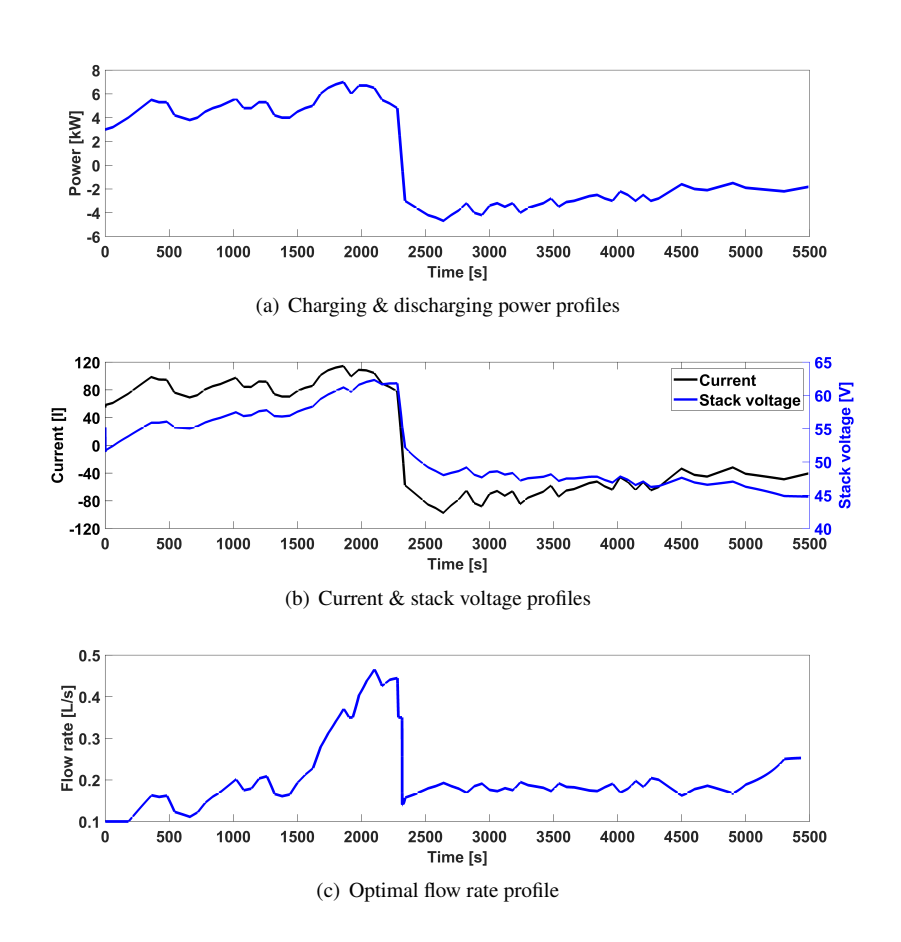


Figure 6: The performance profiles of the 5kW/3kWh VRFB system under a varying power environment obtained by the proposed flow rate control method

simulation study is carried out using a variable charging power from 3kW to 7kW and a variable discharging power from 2kW to 5kW to investigate the energy saving of the proposed method. We assume that the VRFB system was fully balanced at 15% SOC and then charged up to 85%, then discharged to 15% at the end. Another reasonable assumption was learned from [8] and made to reduce the complexities of this optimisation problem: the average current in the last time step remains the same in the next time step, neglecting the small current variations in 1s intervals in this optimisation process.

In Fig. 6 (a), the varying charging/discharging power profiles are shown. The current and stack voltage profiles and the optimal flow rate derived by the proposed method are shown separately in Figs. 6 (b) and (c). It can be seen that the current and stack voltage vary to satisfy the required charging/discharging power, and the derived optimal flow rate varies correspondingly at each time step to minimise energy consumption and maximise energy usage. In this simulation study, the proposed MNDO method achieved 75.08% system efficiency, while the optimal CFR method with FF = 5 reached only 74.51% system efficiency. This means that the proposed method is more efficient by saving energy. Compared to the efficiency gain from the CC

charging/discharging method, a dynamic flow rate control for energy saving becomes necessary in varying power regimes. Even though the efficiency gain is small at 0.57%, it is significant given the considerable amount of energy in medium and large-scale VRFBs. For example, for a 70kWh VRFB with 2000L of electrolyte in each tank under a hypothetical one full cycle per day, the energy savings could be as much as 208kWh in a year. The downside of using the proposed method is the additional computational resources required in industrial applications, which increases the cost to some extent. To address this issue, we propose a simple approach using a 2D lookup table in Section 5 for online applications, which can achieve the same performance without requiring additional resources.

5. DISCUSSION

As described in Section 3, the proposed MNDO method utilises the two energy-saving objectives to determine an optimal flow rate aiming to maximise the system efficiency. The results have been validated in Section 4 to show the superiority and effectiveness of the proposed method in energy saving compared to the CFR control methods under constant and varying current regimes. Several discussions and conclusions are drawn in Sections 4.4 and 4.5 under 100A current in the CC and CC-CV charging modes to analyse the performance of the proposed method and prove the necessity of using the CV charging method to enhance the system efficiency in high-current applications. In this section, several in-depth discussions are presented to explain the reasons behind loss reduction by the proposed optimal flow rate method, the advantages of the CC-CV charging mode in loss reduction, and the underlying benefits of the derived optimal flow rate in active species balancing. More importantly, to create a practical solution for industrial and commercial applications, a simple online flow rate method based on the MNDO approach is proposed and evaluated in this section.

5.1. Performance of the proposed MNDO method in minimising concentration overpotential and pump energy losses

As mentioned in Section 1, the main objective of an optimised flow rate is to dynamically reduce the total losses arising from concentration overpotential and pump energy consumption. We investigate the performance of the proposed method in terms of loss reductions in Fig. 7 under 100A constant charging/discharging cycles.

In Figs. 7 (a) and (b), the overall trend of concentration overpotential and pump energy losses are similar over time, following an exponential function for the proposed method and optimal CFR before 1000s. From 1000s into the simulation until the end of the charging process, however, the optimal flow rate derived by the proposed method is consistently lower to reduce the pump energy consumption. This leads to higher concentration overpotential losses than the optimal CFR control method. Still, the sum of these two losses is lower throughout the charging/discharging cycle in the proposed method, as shown in Fig. 7 (c). It can be observed from Fig. 7 (c) that the total losses are almost the same before 1000s, but the losses obtained from the proposed control method started to reduce after 1000s compared to the CFR method. This proves the necessity to control the flow rate at the late stage of the charging/discharging process to dynamically minimise the sum of these two losses offered by this proposed method. It is worth mentioning that the phenomenon observed in the charging process is not identical to the discharging process. This is caused by the active species on the electrode surface during charging $(V_3^+$ and V_4^+), discharging $(V_2^+$ and V_5^+), and the difference between the variations of

these active species that leads to the difference in concentration overpotential losses showed in Fig. 7 (a). Furthermore, considering the results given in Section 4.4, we can conclude that for a VRFB system with similar configurations and pump design, it is more efficient to utilise a lower flow rate compared with the variable flow rate at the later stage of charging/discharging process to reduce the pump losses. At the later stage of the charging/discharging process, due to the rapid increase of pump power consumption at high speed, a lower flow rate is necessary to reduce the high pump power consumption rather than minimising the concentration overpotential losses. In the early and intermediate stages of the charging/discharging process, the performance of using flow rate control for loss reduction is limited due to the low concentration overpotential losses and pump energy consumption.

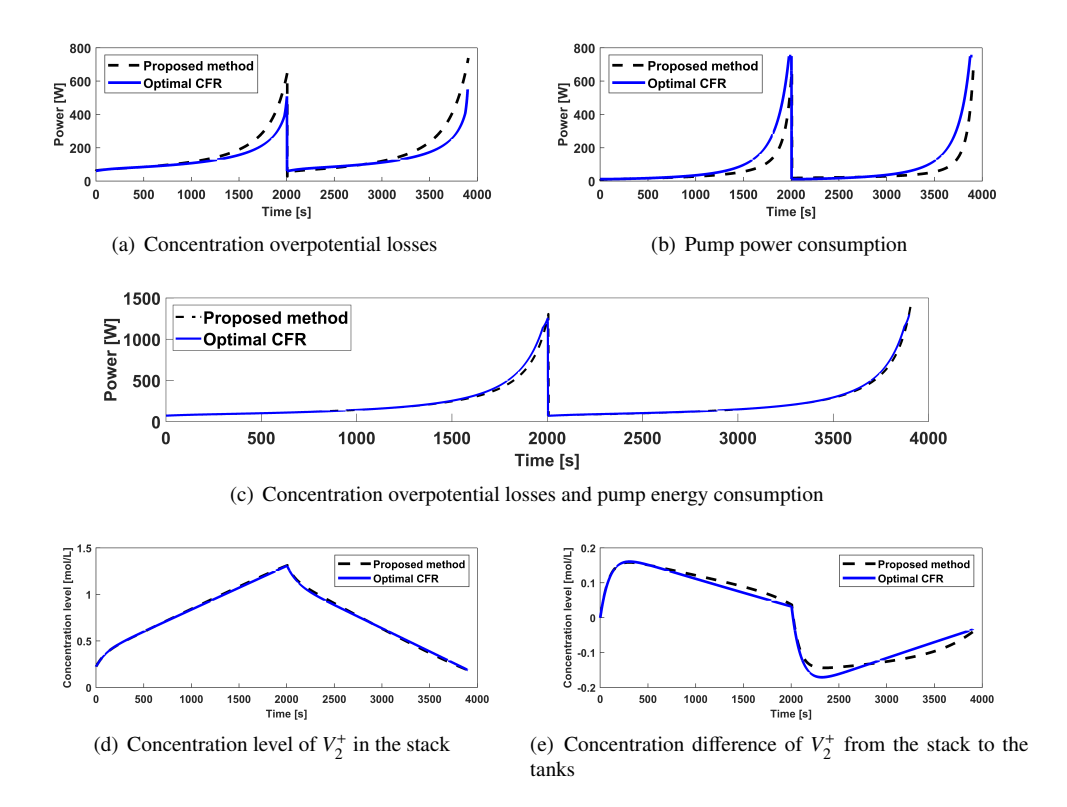


Figure 7: Performance profiles under 100A charging/discharging current by the proposed MNDO method and optimal CFR with FF=5

Furthermore, the concentration level of active species (V_2^+) in the VRFB stack and the concentration difference between the stack and tanks under these two flow rate control methods are given in Figs. 7 (d) and (e). The molarity of the active species almost has no difference between these two methods due to similar flow rate control shown in Fig. 4 (a). However, the result in concentration imbalance from the tank to the stack shows some differences in Fig. 7 (e). It is worth mentioning that the electrolyte flow rate is significant to supply active species to ensure sufficient surface concentration level on the electrodes for electron generation and consumption. A lower concentration imbalance level contributes to balancing the active species and decreases

the concentration overpotential losses. In particular, a lower flow rate contributes to reducing the pump energy consumption but leads to more unbalance between the stack and the tanks.

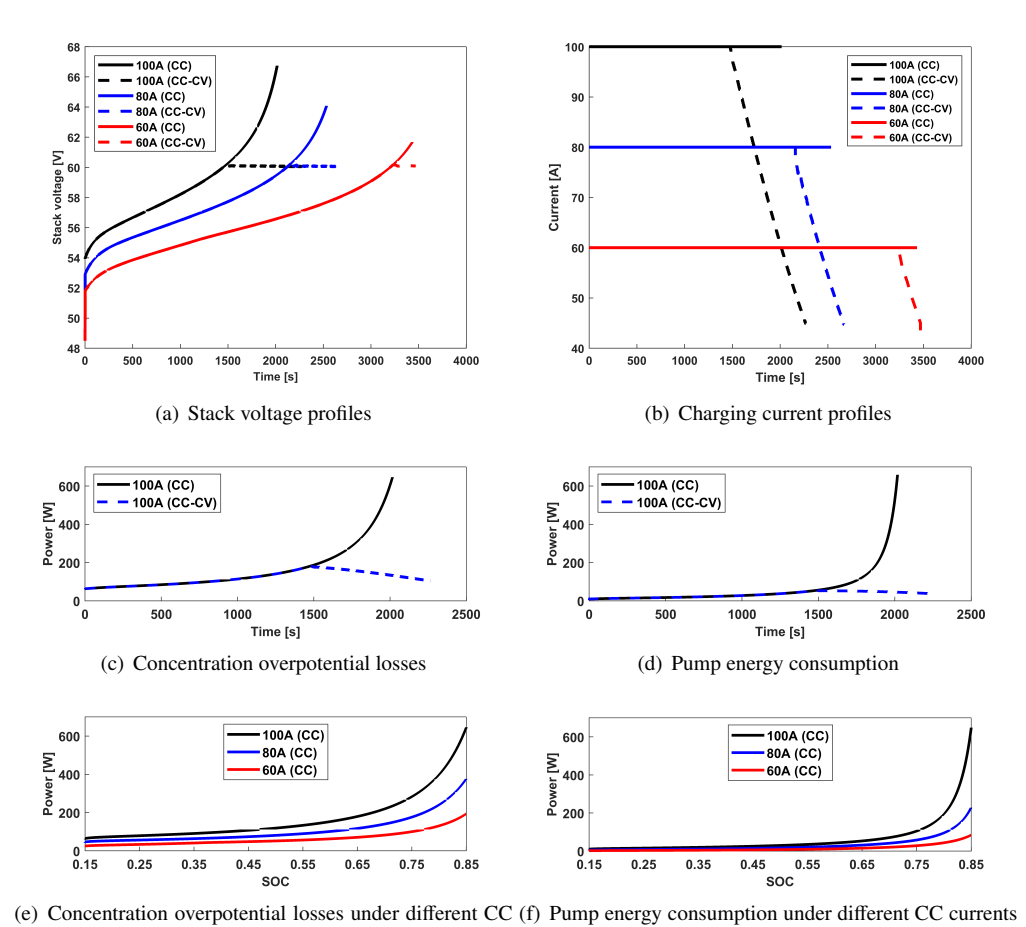
Moreover, the absolute average concentration imbalance level of the optimal CFR and proposed MNDO method is 0.111mol/L and 0.105mol/L, respectively. The total pump power consumption is 0.11kWh and 0.07kWh in the optimal CFR and this proposed MNDO method, respectively. Therefore, the optimal flow rate by the proposed method is more efficient in balancing the active species with a lower pump energy consumption. The reason behind this is that the conventional variable flow rate determined by Faraday's law of electrolysis only determines the flow rate by the number of electrons going into/out of the battery stack and the molarity of actives species in the tanks but neglects the original active species level in the stack which is sufficient for main reactions. Moreover, this proposed method reduces the concentration overpotential by dynamically increasing the flow rate at the early stages of the charging/discharging processes which reduces the concentration imbalance between the stack and tanks. Furthermore, the flow factor in the variable flow rate control methods is determined based on the domain knowledge and expert opinion of a specific VRFB system, mostly neglecting the dynamics of a VRFB system during operation. As a result, a constant flow factor is inefficient in a varying charge/discharge regime and active species variations. In conclusion, the flow rate optimisation process is a complex process that needs to consider the current, active species level, mass transfer coefficient for concentration overpotential losses and pump power consumption under different flow rates. The proposed MNDO method finds an optimal flow rate to maximise efficiency with an accurate VRFB multi-physics model.

5.2. Effects of the CC & CC-CV modes on the performance of VRFB system

To discuss the effectiveness of the CC-CV charging method in saving energy, current and voltage profiles are presented in Figs. 8 (a) and (b) with a charging current of 60A, 80A, and 100A in the CC and CC-CV charging modes. The simulation results of the two charging methods in terms of concentration overpotential and pump energy losses are compared in Figs. 8 (c) and (d) to highlight the loss reduction in the CC-CV charging mode. Another comparison of concentration overpotential and pump energy losses with constant charging currents of 60A, 80A and 100A is shown in Figs. 8 (e) and (f) to emphasise the loss reduction under CC-CV charging mode in high-current applications.

Considering two different charging strategies, the main difference is in the stack voltage and charging current that is due to the charging mode switch as shown in Figs. 8 (a)-(b), which has been discussed in Section 4.5. In both CC and CC-CV modes, a higher charging current results in a higher stack voltage, shown in Fig. 8 (a), due to the rise of ohmic overpotential and concentration overpotential. This leads to a decline in the system efficiency and reduces the voltage efficiency. In Table 4, the system efficiency reduction with respect to the charging current rise demonstrates that the low-current charging will lead to more energy saving during the charging and discharging process as mentioned previously, but charging takes longer.

The CC-CV charging method is introduced to significantly reduce the losses from concentration overpotential and pump operation, as shown in Figs. 8 (c) and (d). These figures indicate that the concentration overpotentials losses and pump power consumption will significantly increase after 70% SOC level, and high losses occur with a high charging current over 80A. Considering that the CC-CV charging method switches from CC to CV after the stack voltage reaches a pre-set limit when the SOC increases to a higher level, the CC-CV charging method saves considerable charging energy in high-current charging applications. This analysis from the per-



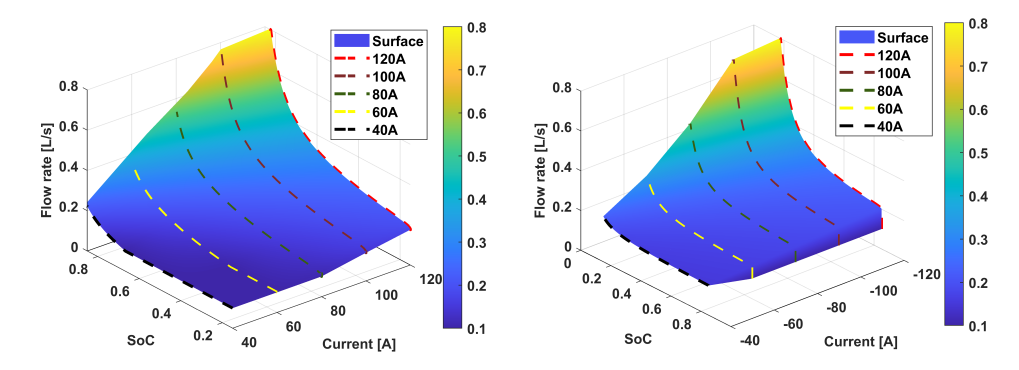
currents vs. SOC vs. SOC

Figure 8: Performance profiles of the $5kW\,/\,3kWh$ VRFB system in different CC and CC-CV scenarios

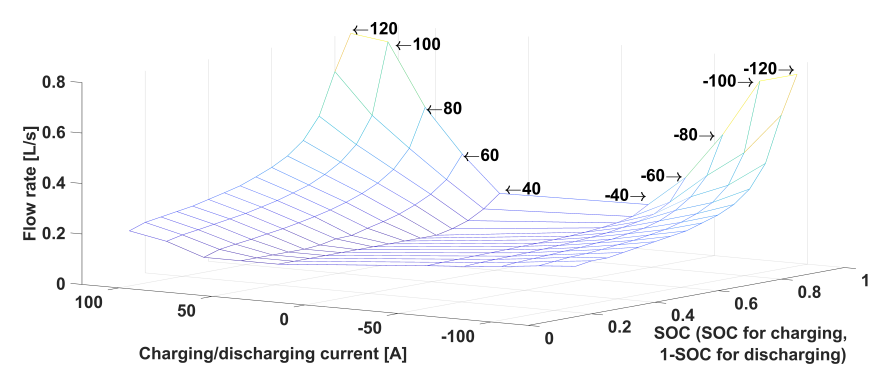
spective of loss reduction supports the conclusion in Section 4.5 and highlights the importance of utilising the CC-CV charging method.

$5.3. \ \ Computationally-efficient\ online\ flow\ rate\ optimisation\ methods\ for\ industrial\ applications$

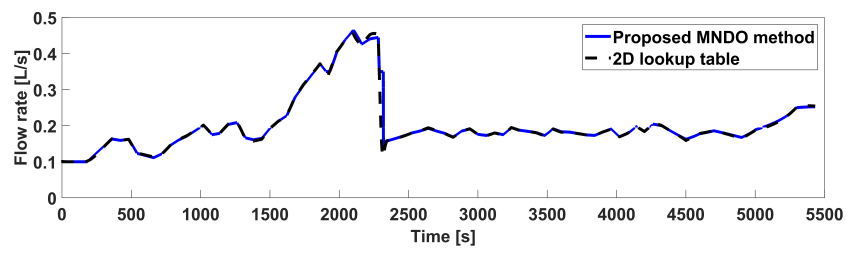
The proposed method in this paper involves repeatedly solving a nonlinear optimisation problem to dynamically find the optimal flow rate during VRFB operation. A similar study considering the dynamic optimisation under a varying power charging/discharging regime has been presented in [10]. It shows an efficiency gain of 0.4% after 30 days. Other studies only considered a constant current operation regime, e.g., [6, 16], also showed limited efficiency gain, mostly around 0.4% in different scenarios. Moreover, for a single variable nonlinear optimisation problem with the constraints in this paper and [6, 16], the optimisation process is fast and does not require significant computational resources. However, it may not be a practical solution in industrial applications with limited computational capability. In [10], the nonlinear optimisation problem has two decision variables with sophisticated nonlinear constraints, which require



(a) Flow rate profiles under the CC mode during charging (b) Flow rate profiles under the CC mode during dischargprocess



(c) Optimal flow rate profiles under the CC mode during discharging process as a 2D lookup table



(d) Performance comparison of the 2D lookup table and the MNDO method in case study $3\,$

Figure 9: A comparison between the optimal flow rates derived by the proposed MNDO method and the 2D lookup table

computationally-intensive solvers, such as particle swarm optimisation or other evolutionary algorithms, to find optimal solutions in real-time.

To avoid solving a nonlinear optimisation problem in real-time, we propose a 2D optimal flow rate lookup table as a function of current and SOC that can be generated from the offline simulation studies. We ran simulation studies for charging currents of 40A, 60A, 80A, 100A and

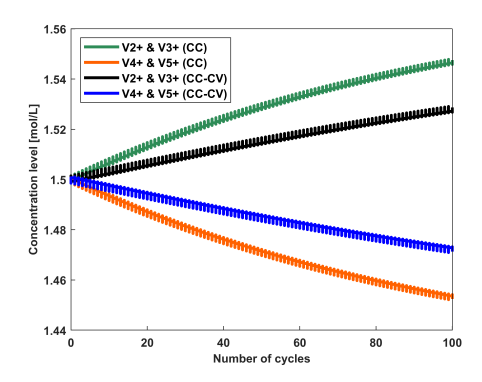
120A with a SOC range from 15% to 85% (Note: the upper SOC limit under 120A charging current is 83.7%). The simulation results are plotted in Figs. 9 (a) and (b) for the charging and discharging process, respectively. Considering the similarities of optimal flow rate under different currents and its impact on energy saving, as was mentioned earlier, a 2D lookup table can be generated for charging and discharging as a function of SOC and current values to dynamically search for the optimal flow rate derived from MNDO methods in constant current scenarios, which is shown in Fig. 9 (c). The SOC is in 5% increments under five different constant currents. The lookup table only contains 15 by 10 datapoints with cubic spline interpolation/extrapolation method, which can be implemented easily in the contemporary BMSs.

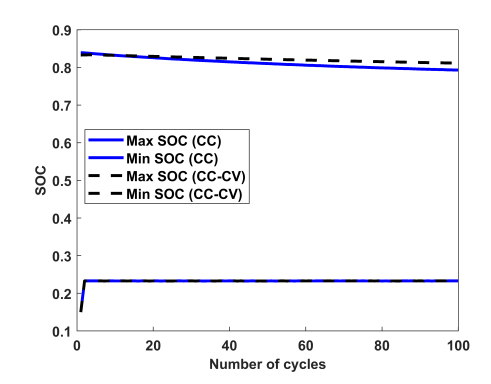
To validate the effectiveness of the proposed 2D lookup table, the varying power regime from Section 4.6 is used along with the 2D lookup table for online flow rate optimisation. The simulation results are compared in Fig. 9 (d), where we can see that the optimised flow rate obtained by the lookup table is almost identical to the values obtained by solving the proposed MNDO optimisation problem. Under the lookup table operation, the system efficiency is 75.08%, which is identical to the previous results. It is worth mentioning that the SOC of the VRFB system is related to the concentration levels of the active species in the stack if the VRFB system is nearly fully balanced and operates under an appropriate flow rate. Moreover, considering the low concentration imbalance in the tanks and stack as shown in Fig. 7 (d), the 2D lookup table will achieve nearly optimal results for energy-saving under a varying power regime. Therefore, we can conclude that using offline simulation studies to create a 2D lookup table can be a practical solution for industry without requiring significant computational resources.

5.4. Evaluating the proposed methods over many operational cycles

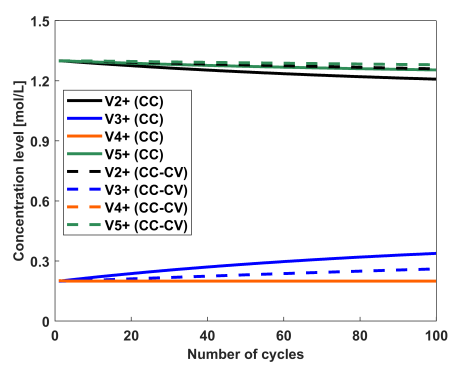
It is well known that VRFB systems suffer from active species imbalances in half-cells after many operational cycles, as mentioned in [18]. The imbalance is caused by the ion diffusion coefficient differences between different active species. After many operational cycles, the electrolyte volume difference in the half-cells of a VRFB will become more significant, thus, resulting in capacity degradation or capacity fading. The phenomenon will result in the increase of $V_2^+ + V_3^+$ in the negative half-cell and the reduction of $V_4^+ + V_5^+$ in the positive half-cell with the Nafion-115 membrane (also known as electrolyte imbalance)[12]. As a result, variations of vanadium species concentrations make flow rate optimisation more complicated. Also, charging methods can exacerbate the difference in active species' imbalance.

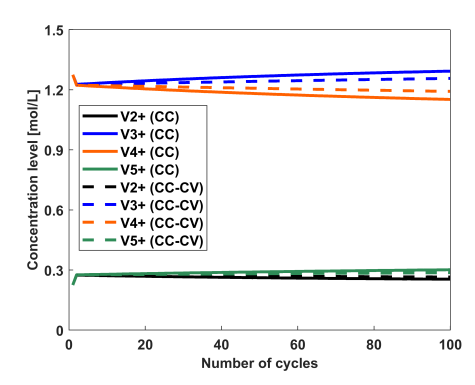
As shown previously, the CC-CV charging method is more energy efficient and requires a lower flow rate compared with the CC charging method. In [6], the authors concluded that a lower flow rate would contribute to reducing capacity fading. Fig. 10 shows the imbalance level of active species in the CC-CV and CC charging mode under 100A constant current discharge over 100 cycles using the proposed method. To avoid the massive reduction of the concentration level of the active species in the stack, which may cause gas evolution and overcharge/over-discharge, the stack voltage limits of the VRFB system are set to 40.4V to 66.6V, which corresponds to cell voltage limits from 1.1V to 1.8V. For the CC-CV charging method, the voltage limits of the VRFB system are set as 40.4V to 60V, and CV is applied after the stack voltage reaches 60V. Notice that to prevent oxygen and hydrogen side reactions, a minimum reactant $(V_3^+$ and V_4^+ for charging, V_2^+ and V_5^+ for discharging) concentration level of 0.2 mol/L in the stack is considered as the operational constraint to protect the VRFB system. This is due to the fact that after long operation, the SOC cannot accurately reflect the concentration level of these four vanadium species caused by imbalance. To ensure the electrode surface concentration is





- (a) Imbalance of the VRFB system in each half cell
- (b) Maximum and minimum SOC profile of the CC-CV and CC charging methods with CC discharging method





(c) Variations of vanadium ions at each end of charging (d) Variations of vanadium ions at each end of discharging processes

Figure 10: Imbalance level and active species variation for the 100A CC & CC-CV charging methods and 100A discharging current over 100 cycles

sufficient at the end of the charging/discharging period, a minimum bulk reactant concentration level is important to prevent the above-mentioned problems.

The results in Fig. 10 (a) show that by using the CC-CV charging mode, the imbalance level is reduced by 40% for both $V_2^+ + V_3^+$ and $V_4^+ + V_5^+$. This is mainly because the CC-CV method utilises a lower average flow rate during the charging process than the CC method, where a lower flow rate can reduce the ion diffusion level, thus reducing the capacity fading [6]. The maximum and minimum SOCs achieved during the charging and discharging process is shown in Fig. 10 (b). It illustrates the benefit of utilising the CC-CV charging method to maximise the capacity of a VRFB system compared with the CC charging mode. The concentration level of the four vanadium species at the end of the charging/discharging process within the 100 cycles is given in Figs. 10 (c) and (d), respectively. In Fig. 10 (c), it is clear that the four vanadium species are more imbalanced in the CC charging mode. Moreover, Fig. 10 (c) shows that the imbalance level of V_3^+ is more significant in the CC charging mode compared with V_5^+ . In Fig. 10 (d), the imbalance level of V_4^+ is slightly larger than V_3^+ . The reactants during the charging and discharging processes

are not used for comparison here due to the physical constraints limiting their variations. This can be explained by the difference in diffusion coefficients where $V_2^+ > V_4^+ > V_5^+ > V_3^+$, and each type of vanadium ions has different variations caused by the difference in the imbalance. In Fig. 10 (c), the reactants of V_4^+ in the CC-CV and CC charging modes are limited to 0.2 mol/L due to their relatively large diffusion coefficient compared with V_3^+ , which leads to the early arrival at the constraints as the overlap in both CC and CC-CV modes. In general, the concentration imbalance is a complicated process that determines the accumulation of vanadium ions in half/negative sides of the VRFB system. These results re-emphasize the necessity of adopting the CC-CV charging mode for reducing active species imbalance and further reducing capacity fading.

As mentioned previously, due to the imbalance of active species in the VRFB half-cells, the proposed MNDO method and 2D lookup table performance may not be efficient enough to handle the optimisation problem under a varying active species environment. To evaluate the system efficiency enhancement using the proposed methods, a case study is performed using the CC-CV and CC charging methods at 100A current and 60V voltage limit, the same as the previous setting, with a discharging current of 100A for 100 cycles. The system efficiency results of the three methods are given in Table 5. In this table, the proposed MNDO method yields an efficiency improvement of up to 0.99% compared with the optimal CFR method in CC charging mode, and an efficiency gain of 0.43% is also achieved in CC-CV charging scenario. Furthermore, the lookup table's performance is the same as the proposed MNDO method in the CC-CV charging scenario of 100 cycles. Note that there is a slight system efficiency gain by the proposed 2D lookup table compared to the results obtained by the proposed MNDO method in 100 cycles. This is achieved by the 2D lookup table not being able to charge the VRFB system to a higher SOC level during the charging process, thus achieving a better performance in loss reduction from concentration overpotentials and pump power consumption. Most importantly, combining these two proposed methods with the CC-CV charging can result in a considerable system efficiency gain of up to 1.48% compared with CC charging and the CFR control method. Please note that the 2D lookup table is not available under the CC charging mode below 100 cycles because of the significant imbalance which caused several limitations in simulation. This is caused by the lack of a usable mapping relationship between optimal flow rate and active species level after 100 cycles. After long-term continuous operation, the concentration imbalance in the half-cells becomes more significant, and thus the lookup table design is not usable in this case when the concentration variations become more rapid at the later stage of the charging/discharging processes. Considering the benefits of using the CC-CV charging in reducing the imbalance and energy saving, lookup table approach and the CC-CV charging method can be advised for an online optimal flow rate control within 100 cycles. Normally the lifespan of a VRFB system can be more than 10,000 cycles, and the capacity can be restored by simply rebalancing the electrolyte using regeneration cells or continuous overflow[19, 20, 21]. It is worth mentioning that the proposed method is able to cope with different current regimes as we validated in our study. The use of CC-CV in charging is recommended but its use depends on the demands of customers and the actual operational environment.

This study proves the effectiveness of using the proposed optimisation method and its equivalent lookup table to control the electrolyte flow rate to save energy. However, it should be noted that control of the flow rate has a limited impact on the efficiency of a VRFB system. Furthermore, running simulation studies with the proposed MNDO method for a specific VRFB system and generating a lookup table with a small data sample can efficiently control the flow rate without additional computational resources.

Table 5: System efficiency of the CC-CV and CC charging under 100 A and CC discharging for 100 cycles

Methods	CC-CV	CC
Optimal CFR	71.28%	70.24%
Optimal CFK	(FF=5)	(FF=6)
Proposed MNDO method	71.71%	71.23%
Proposed 2D lookup table	71.72%	Not available

6. CONCLUSIONS

A dynamic multi-physics and hydraulic model of a 5kW/3kWh VRFB system is developed to simulate the VRFB operation under different current profiles and flow rates, and validated by experimental data in the CC mode. Then, a model-based nonlinear dynamic optimisation method is proposed to optimise the flow rate in real-time aiming to maximise energy usage. The results have shown that the proposed MNDO method can indeed maximise the system efficiency under the given objectives. Detailed simulation studies and discussions have been presented in this paper to analyse various aspects of the system operation in depth. The key findings in this paper are as follows:

- The simulation results show an improvement in the system efficiency when the proposed MNDO method is used in comparison with the optimal CFR methods.
- The CC-CV charging mode is adopted for VRFBs to enhance the system efficiency under a
 high-current charging application and the feasibility of this proposed dynamic optimisation
 method is proved under varying power regimes.
- The loss reduction by electrolyte flow rate control is analysed, and the benefit of using the CC-CV charging method in reducing system imbalance and improving system efficiency is highlighted.
- A computationally efficient and practical 2D lookup table is designed based on the simulation results obtained from the proposed MNDO method. Then, the performance of these two methods is evaluated within 100 cycles.

For future work, an in-depth analysis of the influence of electrolyte flow rate in capacity fading and system imbalance is necessary to develop an efficient method to enhance the system energy efficiency of a VRFB system while reducing capacity degradation. Meanwhile, the design of efficient and reliable imbalance observers is crucial to estimate the imbalance level based on other simple-to-measure parameters, e.g., stack voltage, SOC, etc, to enhance the performance of the lookup table design.

ACKNOWLEDGEMENTS

Funding for a PhD scholarship is provided by the Microgrid Battery Deployment project, which is funded by the Future Battery Industries Cooperative Research Centre as part of the Commonwealth Cooperative Research Centre Program, Australia.

References

- [1] Hao Wang, S Ali Pourmousavi, Wen L Soong, Xinan Zhang, and Nesimi Ertugrul. Battery and energy management system for vanadium redox flow battery: A critical review and recommendations. *Journal of Energy Storage*, 58:106384, 2023.
- [2] Ao Tang, Jie Bao, and Maria Skyllas-Kazacos. Studies on pressure losses and flow rate optimization in vanadium redox flow battery. *Journal of Power Sources*, 248:154–162, 2014.
- [3] Xiangkun Ma, Huamin Zhang, Chenxi Sun, Yi Zou, and Tao Zhang. An optimal strategy of electrolyte flow rate for vanadium redox flow battery. *Journal of Power Sources*, 203:153–158, 2012.
- [4] Binyu Xiong, Jiyun Zhao, K.J. Tseng, Maria Skyllas-Kazacos, Tuti Mariana Lim, and Yu Zhang. Thermal hydraulic behavior and efficiency analysis of an all-vanadium redox flow battery. *Journal of Power Sources*, 242:314–324, 2013
- [5] A Karrech, K Regenauer-Lieb, and F Abbassi. Vanadium flow batteries at variable flow rates. *Journal of Energy Storage*, 45:103623, 2022.
- [6] S König, MR Suriyah, and T Leibfried. Innovative model-based flow rate optimization for vanadium redox flow batteries. *Journal of Power Sources*, 333:134–144, 2016.
- [7] Yifeng Li, Xinan Zhang, Jie Bao, and Maria Skyllas-Kazacos. Studies on optimal charging conditions for vanadium redox flow batteries. *Journal of Energy Storage*, 11:191–199, 2017.
- [8] Md Parvez Akter, Yifeng Li, Jie Bao, Maria Skyllas-Kazacos, and Muhammed Fazlur Rahman. Optimal charging of vanadium redox flow battery with time-varying input power. *Batteries*, 5(1):20, 2019.
- [9] Tossaporn Jirabovornwisut, Soorathep Kheawhom, Yong-Song Chen, and Amornchai Arpornwichanop. Optimal operational strategy for a vanadium redox flow battery. Computers & Chemical Engineering, 136:106805, 2020.
- [10] Tao Wang, Jiahui Fu, Menglian Zheng, and Zitao Yu. Dynamic control strategy for the electrolyte flow rate of vanadium redox flow batteries. Applied Energy, 227:613–623, 2018.
- [11] Bahman Khaki and Pritam Das. Multi-objective optimal charging current and flow management of vanadium redox flow batteries for fast charging and energy-efficient operation. *Journal of Power Sources*, 506:230199, 2021.
- [12] Ao Tang, Jie Bao, and Maria Skyllas-Kazacos. Thermal modelling of battery configuration and self-discharge reactions in vanadium redox flow battery. *Journal of Power Sources*, 216:489–501, 2012.
- [13] Yifeng Li. Advanced Modelling, Optimisation and Control of Vanadium Redox Flow Battery. PhD thesis, The University of New South Wales, 2018.
- [14] Yifeng Li, Maria Skyllas-Kazacos, and Jie Bao. A dynamic plug flow reactor model for a vanadium redox flow battery cell. *Journal of Power Sources*. 311:57–67, 2016.
- [15] S Corcuera and M Skyllas-Kazacos. State-of-charge monitoring and electrolyte rebalancing methods for the vanadium redox flow battery. European Chemical Bulletin, 1(12):511–519, 2012.
- [16] Edison Banguero, Antonio Correcher, Angel Perez-Navarro, Francisco Morant, and Andres Aristizabal. A review on battery charging and discharging control strategies: Application to renewable energy systems. *Energies*, 11(4):1021, 2018.
- [17] Bahman Khaki and Pritam Das. An equivalent circuit model for vanadium redox batteries via hybrid extended kalman filter and particle filter methods. *Journal of Energy Storage*, 39:102587, 2021.
- [18] Ao Tang, Jie Bao, and Maria Skyllas-Kazacos. Dynamic modelling of the effects of ion diffusion and side reactions on the capacity loss for vanadium redox flow battery. *Journal of Power Sources*, 196(24):10737–10747, 2011.
- [19] Nicola Poli, Michael Schäffer, Andrea Trovò, Jens Noack, Massimo Guarnieri, and Peter Fischer. Novel electrolyte rebalancing method for vanadium redox flow batteries. *Chemical Engineering Journal*, 405:126583, 2021.
- [20] Arjun Bhattarai, Purna C Ghimire, Adam Whitehead, Rüdiger Schweiss, Günther G Scherer, Nyunt Wai, and Huey Hoon Hng. Novel approaches for solving the capacity fade problem during operation of a vanadium redox flow battery. *Batteries*, 4(4):48, 2018.
- [21] Katharina Schafner, Maik Becker, and Thomas Turek. Capacity balancing for vanadium redox flow batteries through continuous and dynamic electrolyte overflow. *Journal of Applied Electrochemistry*, 51(8):1217–1228, 2021.